Proceedings of the Canadian Society for Mechanical Engineering International Congress
32nd Annual Conference of the Computational Fluid Dynamics Society of Canada
Canadian Society of Rheology Symposium
CSME-CFDSC-CSR 2025
May 25–28, 2025, Montréal, Québec, Canada

Geometrical Investigation of Solar Chimney with PCM-Integrated Trombe Wall for Enhanced Thermal Comfort and Energy Efficiency

Nima Ghorbani[1*], Amirhossein Khayyaminejad [1], Mahdiyar Khalilzade Shabestari[1], Amir Fartaj[1]
[1]Department of Mechanical, Automotive, and Materials Engineering, University of Windsor, Windsor, Ontario, Canada
*Ghorbni@uwindsor.ca

Abstract—The global rise in population and energy demand has amplified environmental challenges such as resource depletion, pollution, and escalating fuel prices, underscoring the critical need for sustainable and renewable energy solutions. Sustainable design principles aim to address these challenges by promoting energy-efficient systems and reducing the environmental footprint of buildings. Among these strategies, passive solar systems, such as Solar Chimneys (SC) and Trombe Walls (TW) integrated with Phase Change Materials (PCM), demonstrate significant potential for improving energy efficiency and indoor thermal comfort. This study examines the combined effects of TW-PCM and vertical SC on indoor temperature and heating load in the hot and humid climate of Rio de Janeiro, utilizing DesignBuilder 7.0.2 and EnergyPlus simulation tools. The research evaluates various solar chimney configurations, focusing on height (5 m, 6.5 m, and 8 m), outlet surface area (1.5 m², 2.5 m², and 3.5 m²), and shapes (square, pentagon, and hexagon) to determine optimal geometric configurations for sustainable building performance. Increasing the solar chimney height to 8 m significantly enhanced indoor thermal performance, raising the average indoor temperature to 23.15°C and reducing the average heating load to 169.7 kWh. Peak heating loads of 335 kWh were recorded during the winter month of July, specifically from the 18th to the 21st. Expanding the outlet surface area to 3.5 m² further improved performance, achieving an average indoor temperature of 23.65°C and reducing the average heating load to 118.8 kWh. This configuration extended the mechanical-free operation period by 26 hours compared to the height scenario, highlighting its efficiency in enhancing passive operation. However, the most impactful improvement was achieved by modifying the solar chimney to a 6-sided (hexagonal) configuration. This design increased the average indoor temperature to 24.2°C, reduced the peak heating load to 212.5 kWh, and achieved a significantly lower average heating load of 48.9 kWh. Furthermore, the hexagonal configuration extended the passive operation period by an additional 9 hours compared to the expanded outlet surface area scenario. These findings underscore the importance of geometric optimization in solar chimney design for achieving superior thermal performance, reduced energy consumption, and extended passive operation periods. Incorporating passive solar systems into sustainable building designs provides an effective strategy for addressing energy challenges while enhancing indoor comfort. By optimizing the geometry of solar chimneys, this study contributes valuable insights to the development of innovative, energy-efficient, and environmentally sustainable building solutions.

Keywords: Solar Chimney; Trombe Wall; Passive Heating; PCM; Sustainable Design; Renewable Energy

I. INTRODUCTION

The global population continues to grow rapidly, driving an escalating demand for energy that places immense pressure on traditional fuel reserves such as oil, gas, and coal. This dependence on finite fossil fuels not only accelerates resources exhaustion but also exacerbates environmental degradation and contributes to volatile, rising fuel prices [1]. With projections suggesting the depletion of conventional energy reserves within the next half-century, the urgency to shift toward sustainable, clean energy alternatives has never been more critical [2]. Considering that conventional energy sources are widely used and consumed continuously, they are expected to be depleted within the next fifty years. The current global energy challenges are among the most urgent issues, which has led scientists and engineers to seek new, renewable, and environmentally friendly energy sources [3,4]. These efforts resulted in the emergence of the concept of renewable energy, which includes sources like solar energy, wind energy, hydroelectric power, ocean and sea energy, geothermal energy, and more [5]. To decrease pollution and enhance human and economic development, generating power from renewable energy sources, like solar energy, is critically important [6].

Passive solar heating and ventilation systems, such as solar roofs, Solar Chimney, and Trombe Wall, have demonstrated improvements in energy efficiency. These systems can achieve annual energy savings ranging from 30% to 70%, influenced by factors like wall size, orientation, insulation quality, glazing materials, and local climate conditions. Natural ventilation can effectively enhance thermal comfort and reduce energy consumption in residential buildings. Research shows that homes with SCs experience a notable reduction in daily air-conditioning energy use, approximately 10% to 20% less than conventional spaces. Furthermore, when operating optimally, SCs can lower operating costs by up to 30%. The passive heating mechanism functions by using buoyancy to move warm air upward, creating a natural flow from the inlet to the outlet, where cooler, denser air replaces the rising warm air, ensuring continuous circulation. This process, which includes radiation, convection, and conduction, improves indoor comfort while decreasing reliance on non-renewable heating sources.

Numerous researchers have explored the efficiency of SC and their influence on Indoor Air Quality (IAQ). Ahmed et al. [7] conducted a thorough investigation into the effectiveness of SC in residential buildings, focusing on identifying the key parameters influencing their ventilation performance. Rabani et al. [8] investigated the performance of inclined SCs in hot and arid climates. Their experiments demonstrated that utilizing a SC could lower room temperatures by as much as 14°C. Shi et al. [9] examined various SC designs, including inclined, glazed, and rooftop models. Following this, Shi et al. [10] developed a mathematical model to predict the performance of SC by considering factors such as inclination angle, height, width, and the size of the inlet and outlet areas. However, the majority of their test results were derived under indoor conditions. In 2016, Ahmed Abdeen Saleem et al. [11] demonstrated that their proposed SC designed with a 45° inclination, 1.4 m length, 0.6 m width, and a $0.20\ m$ air gap, achieved an airflow rate aligning with ASHRAE Standard 62 ($0.019\ to\ 0.033\ m^3/s$). The system exhibited 88.2% effectiveness during daytime, highlighting its potential for improving indoor air quality in hot, arid climates. Khayyaminejad and Fartaj [12] demonstrated that incorporating a PCM layer into a building with a SC enhanced energy savings by 5% during peak temperatures and by 3.5% over a 24-hour period, compared to a building without Phase Change Material integration.

Passive solar systems are an effective means of enhancing the energy efficiency of buildings [13–16]. A TW is a passive solar system with indirect heat gain, designed to enhance the material's capacity to absorb, store, and release heat through heat transfer processes. The traditional TW consists of a massive interior wall made of materials with high heat storage capacity, followed by an air layer and an outer glazing. Over the years, numerous studies have been conducted to evaluate the performance of TW. Innovative concepts have emerged, focusing on factors such as the materials used for the massive wall [16–22], the type of glazing [23], the design of ventilation openings, and the incorporation of thermal insulation. In 1987, Drake [24] improved heat capacity by integrating PCM wallboards. Later, Peippo et al. [25] identified that the optimal melting point for PCM should be $1-3°C$ above the average room temperature. Kong et al. [26] studied a TW system incorporating single and dual layers of microencapsulated PCMs under summer and winter conditions, evaluating four operational modes for heating and ventilation. Their findings revealed that dual PCM layers reduced the average room temperature by $0.9°C$ in summer and increased it by $6.6°C$ in winter, while heat flux was decreased by up to 92% in summer and 75.7% in winter.

This study presents a unique exploration of the integration of TW with PCM and vertical SC to assess their combined effects on indoor temperature and energy efficiency in the hot and humid climate of Rio de Janeiro. This study focuses on analyzing the impact of varying geometric parameters of a solar chimney, including its height, outlet surface area, and different shapes of SC, to evaluate their influence on the indoor temperature of a house during the winter. A major contribution of this study is the identification of the optimal SC geometry that maximizes the benefits of the TW-PCM and SC integration, providing valuable insights for optimizing building designs to enhance energy efficiency and occupant comfort. The findings provide a foundation for future studies on integrating renewable energy systems with HVAC solutions, emphasizing their potential to enhance energy efficiency and indoor comfort in sustainable building design.

II. Methodology

The study focuses on a physical domain configuration located in Rio de Janeiro, with geographic coordinates approximately 22.9° S latitude and 43.2° W longitude, Rio de Janeiro experiences a hot and humid climate, with winter temperatures generally ranging from a minimum of around $18°C$ to highs exceeding $26°C$. The average wind speed in the city is approximately $3.4\ m/s$. The mean global solar radiation in Rio de Janeiro is approximately $5.5\ kWh/m^2$ per day. The studied domain covers a square area of 100 m² with a height of $4\ m$. It features fenestrations facing east and west, each with an area of $6\ m^2$. The set-point temperature used for calculating heating loads is maintained at $23\ °C$. A SC is installed on the northern facade, while a TW integrated with PCM is placed on the southern facade.

The TW integrated with PCM is installed on the exterior wall. Placing the TW on the exterior wall of a large, open space greatly improves its performance by enabling more effective natural ventilation over a wider area. The exterior layer consists of lightweight metallic cladding with a thickness of 0.01 m, followed by an air gap measuring $0.5\ m$. The interior surface is finished with a gypsum plaster layer that is $0.05\ m$ thick. The roof's exterior layer is made of asphalt with a thickness of 0.05 m. For the floor on soil, the interior layer includes timber flooring, followed by a floor screed with thicknesses of $0.03\ m$ and $0.07\ m$, respectively. To enable buoyancy-driven airflow, outdoor air enters the air gap through a lower opening, where it is heated before rising and flowing into the building through an upper opening. A schematic diagram of the TW is shown in Figure 1. The TW design includes an air gap and is equipped with four grilles: two located near the ceiling and two positioned near the floor. In this study, the PCM used is Infinite RPCM $18°C$. The PCM has a thermal conductivity of $0.815\ W/m \cdot K$ and a density of $929\ kg/m^3$. It operates using a hysteresis phase change method. In its liquid state, the PCM demonstrates a thermal conductivity of 0.54 W/m·K, a density of $1540\ kg/m^3$, and a specific heat capacity of $3140\ J/kg \cdot K$.

The vertical, square-shaped SC features a glass wall oriented towards the north wall. It has a surface area of 4 m² and a height of 5 m. Inside the SC, there is a central wall with a surface area of $10.8\ m^2$ and a height of $4\ m$. This wall is composed of three layers: two aluminum absorber walls on the outer sides and an Expanded Polystyrene insulating layer sandwiched between them. The aluminum absorber walls, known for their high thermal conductivity of approximately $237\ W/m \cdot K$, ensure efficient heat transfer. In contrast, the EPS insulation layer, with its low thermal conductivity of about 0.035 $W/m \cdot K$, offers excellent thermal resistance, effectively reducing heat loss between the two absorber layers. This study investigates the impact of SC geometry on indoor temperature by varying its structural configuration and analyzing the resulting effects on indoor temperature distribution and heating load requirements.

A. Height

The effect of SC height on indoor temperature was analyzed by adjusting its height to 5 m (original model), 6.5 m, and 8 m. In each scenario, the glazing surface area and the absorber plate surface area within the SC were modified accordingly, leading to variations in indoor temperature. At a height of 6.5 m, the solar chimney incorporates $32.5m^2$ glazing and $17.875m^2$ absorber, while at a height of 8 m, it features $40m^2$ glazing and $22m^2$ absorber.

B. Outlet Surface Area

The effect of the SC's outlet surface area on indoor temperature was examined by adjusting the outlet size to 1.5 m^2 (original model), 2.5 m^2, and 3.5 m^2. In each configuration, both the glazing surface area and the absorber plate surface area within the SC were modified accordingly, resulting in distinct variations in indoor temperature and heating load. At an outlet area of 1.5 m^2, the SC includes $25m^2$ glazing and $13.75m^2$ absorber, while at 2.5 m^2, it incorporates $31m^2$ glazing and $15.5m^2$ absorber, and at 3.5 m^2, it features $42m^2$ glazing and $20m^2$ absorber.

C. SC shapes

The influence of varying the number of SC sides on indoor temperature and heating load was investigated by changing the configuration from square-shape (original model) to pentagon and hexagon. Figure 2 shows each scenario involved adjustments to the glazing surface area and absorber plate surface area, as well as changes in the number of glazing and absorber panels. These modifications resulted in distinct indoor temperature fluctuations and heating load variations. In the 4-sided configuration, the SC includes $25m^2$ glazing panels and $13.75m^2$ absorber panels; in the 5-sided configuration, it features $40m^2$ glazing panels and $18.75m^2$ absorber panels; and in the 6-sided configuration, it incorporates $36m^2$ glazing panels and $29.25m^2$ absorber panels.

In configuring the SC and TW within the DesignBuilder 7.0.2 simulation tool, the solar distribution setting was defined as 'Full Interior and Exterior' to ensure accurate modeling of sunlight interactions with both the exterior and interior surfaces of the TW. Additionally, the zone type was set to 'Cavity', enabling the precise simulation of the SC and TW as solar heat collectors. The simulations utilized the EnergyPlus engine, validated through multiple experimental studies [30]. For scenarios without PCM, the Conduction Transfer Function (CTF) method was applied, accurately modeling radiation, convection, conduction, and air and moisture transfer. Conversely, for PCM simulations, the Finite Difference Method was employed, focusing exclusively on heat transfer and excluding moisture effects, using a fully implicit first-order scheme known for its stability despite slower computational performance [30]. The analysis was conducted for the winter week of July 18th to 21st, based on Rio de Janeiro weather data, with a focus on solar-driven natural ventilation to enhance comfort, while minimizing energy consumption and operational costs associated with continuous mechanical conditioning systems.

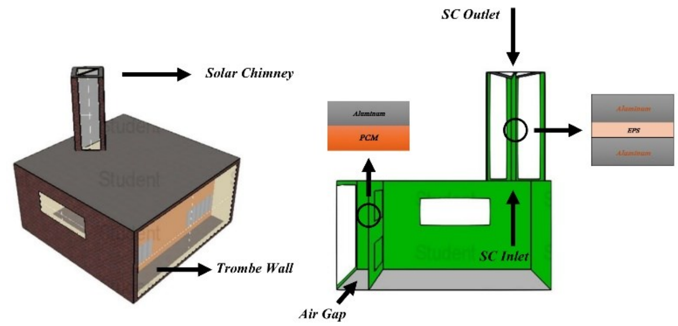

Figure 1. Model Layout

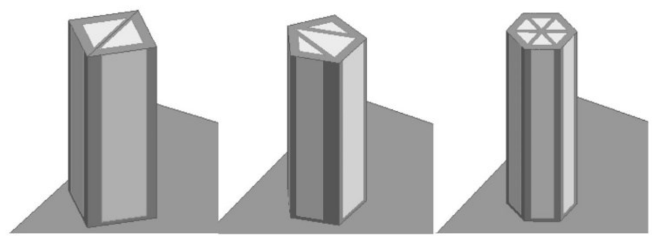

Figure 2. SC different shapes

III. VALIDATION

The validation of the SC is illustrated in Figure 3, where the accuracy of the numerical simulations in this study is compared to the mathematical and numerical data from Saleem et al. [11]. Saleem et al.'s work, conducted under conditions similar to those studied by Mathur et al. [28] and Imran et al. [11], serves as a reference for validation. Imran et al. [29] carried out experiments in a room measuring $2\,m \times 3\,m \times 2\,m$, equipped with a SC featuring a 1 mm aluminum collector wall, a 4 mm glass panel, and adjustable air gap thicknesses and tilt angles. A detailed comparison of the numerical results from this study with Saleem et al. [7], as presented in Figure 4, demonstrates a strong correlation, validating the reliability of the simulations. The maximum observed error was 1.9% at hour 3.

Figure 4 illustrates the validation of the TW. The experimental study conducted by Zhang et al. [27] was selected to verify the accuracy of the numerical simulations. In their experiment, a TW was installed on the southern wall of a building, with data collected from April 23rd to April 25th. The study also integrated PCM into the TW to evaluate their effect. As shown in Figure 3, the numerical results are in close agreement with the experimental data, with a maximum error of 1.27% observed on April 26th at 10:00 PM.

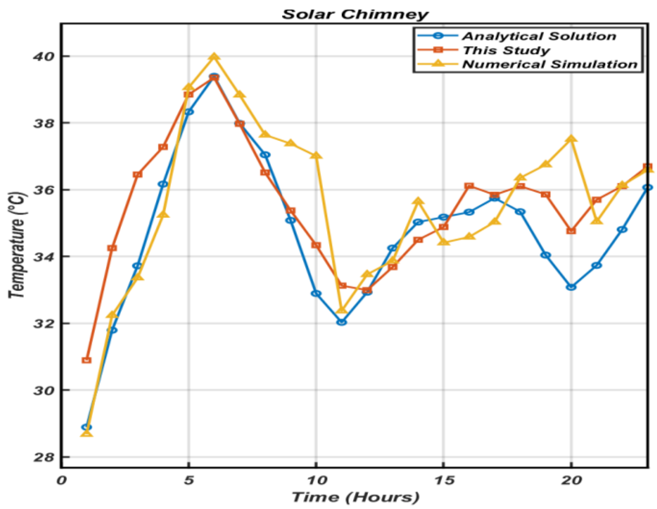

Fig. 3: SC simulation validation [11].

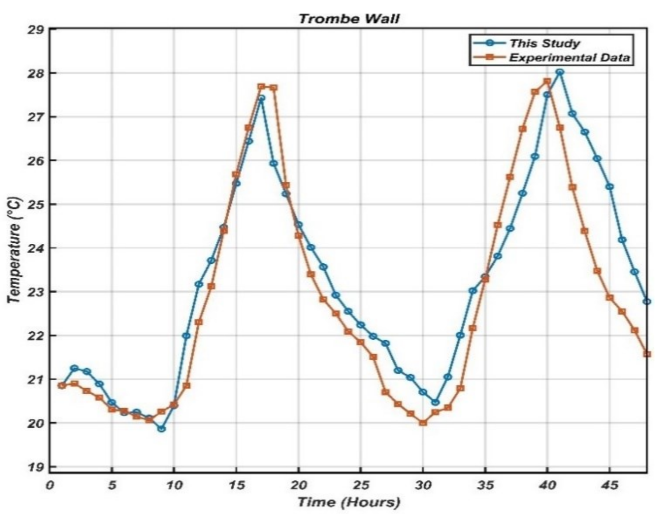

Fig. 4: TW simulation validation [27].

IV. Results and Discussion

A. *Effect of Height*

Figure 5. (a) illustrates the indoor temperature variations observed at different SC heights. The yellow line represents the scenario with a $5m$ (original model) height SC, where indoor temperatures fluctuate between $20°C$ and $26°C$, with a peak temperature of $25.9°C$ and a minimum of $20.2°C$. In the second scenario, where the SC height is increased to 6.5 meters (depicted by the red line), the peak indoor temperature rises by $0.5°C$, with an average temperature of approximately $22.8°C$. In the third scenario, represented by the blue line, the SC height is extended to 8 meters, leading to a peak temperature increase of $1.2°C$ and an average temperature of around $23.2°C$. The analysis indicates that the 8-meter SC has the most significant impact on indoor temperature performance due to an increase in glazing and absorber surface area.

B. *Effect of Outlet Surface Area*

Figure 5. (b) demonstrates that increasing the surface area of the SC has a more pronounced effect on indoor temperature compared to height adjustments because it leads to a significant increase in glazing area which improves the SC performance. The yellow line represents the scenario with a $1.5\ m^2$ outlet surface area, where the average indoor temperature stabilizes around $22.6°C$. In the second scenario, where the outlet surface area is increased to 2.5 m² (illustrated by the red line), the peak indoor temperature rises by $0.7°C$, with an average temperature of approximately $22.9°C$. The third scenario, shown by the blue line, features a $3.5\ m^2$ outlet surface area, resulting in a peak temperature increase of $1.9°C$ and an average indoor temperature of around $23.6°C$. The temperature fluctuates between a peak of $27.9°C$ and a minimum of $20.8°C$ in this configuration. The findings clearly indicate that a SC with a $3.5\ m^2$ surface area has a greater impact on increasing indoor temperature compared to modifications in the chimney height.

C. *Effect of the SC shapes*

Figure 5. (c) highlights that increasing the number of sides of the SC has a more significant effect on indoor temperature compared to adjustments in height or outlet surface area. The yellow line represents the scenario with a square shape SC, where the average indoor temperature stabilizes around $22.6°C$. In the second scenario, with the number of sides increased to 5 (pentagon shape) (depicted by the red line), the peak indoor temperature rises by $0.8°C$, resulting in an average temperature of approximately $23.1°C$. The third scenario, shown by the blue line, involves a hexagon shape SC, leading to a peak temperature increase of $2.2°C$ and an average indoor temperature of around $24.2°C$. In this configuration, temperatures fluctuate between a peak of $26.9°C$ and a minimum of $21.6°C$. The results demonstrate that a hexagon shape SC exerts a more substantial influence on indoor temperature performance, primarily due to the increase in the number of absorber plates and glazing surfaces, which enhance heat absorption and distribution efficiency.

D. *Heating Load*

Figure 5. (d) presents a comparative analysis of heating load performance across different SC configurations. In Case 1, where the SC height was increased to 8 meters, the heating load peaked at approximately $335\ kWh$, with an average heating load of $169.7\ kWh$. In Case 2, where the surface area was expanded to 3.5 m², the peak heating load rose to around $370\ kWh$, while the average heating load decreased to $118.8\ kWh$, extending the period without mechanical heating systems by approximately 26 hours compared to Case 1. In Case 3, representing a hexagon shape SC, the heating load decreased significantly, with an average value of approximately $48.9\ kWh$ and a peak load of around $212.5\ kWh$, further extending the system's passive operation period by an additional 9 hours compared to Case 2. These results demonstrate that increasing the number of sides of the SC is the most effective strategy for reducing heating loads, enhancing thermal comfort, and promoting energy efficiency, underscoring the value of sustainable design and passive heating approaches in optimizing building energy performance.

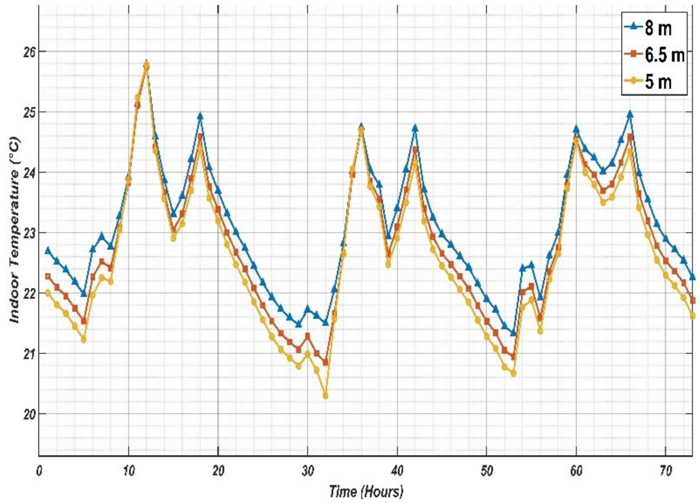

(a)

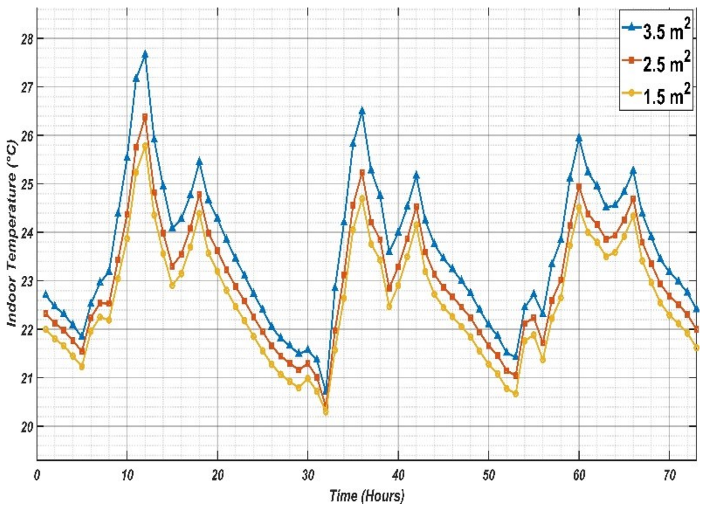

(b)

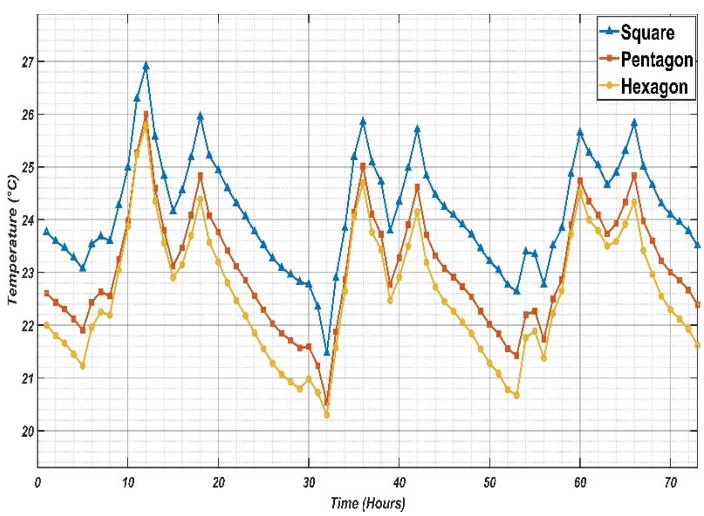

(c)

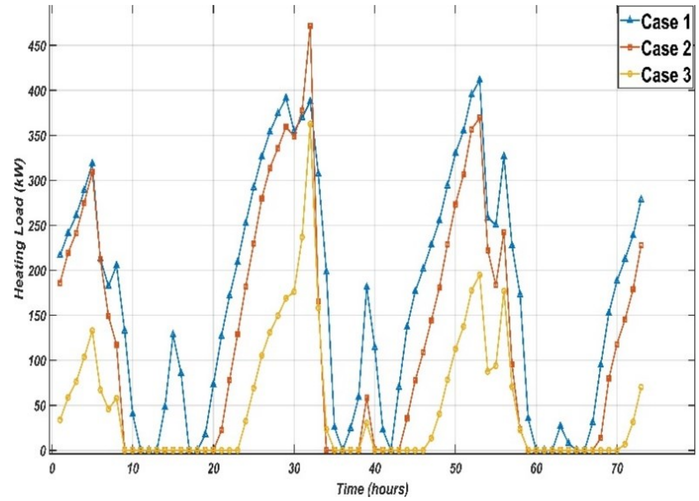

(d)

Figure 5. Indoor air temperature in different scenarios (a) different height, (b) different outlet surface area, (c) different number of sides, (d) heating load

V. Conclusion

This study investigated the combined effects of SC and TW integrated with PCM on indoor temperature and heating load performance in a hot and humid climate, specifically in Rio de Janeiro. Using numerical simulations conducted in DesignBuilder 7.0.2 with the EnergyPlus engine, the study evaluated the impact of varying SC height $(5\ m, 6.5\ m, and\ 8\ m)$, outlet surface area $(1.5\ m^2, 2.5\ m^2, and\ 3.5\ m^2)$, and the shape of SC (square, pentagon, hexagon) on energy efficiency and thermal comfort.

The results revealed that increasing the SC height to 8 m raised the average indoor temperature to $23.15°C$, with a peak heating load of $335\ kWh$ and an average heating load of $169.7\ kWh$. Adjusting the outlet surface area to $3.5\ m^2$ improved the average indoor temperature to $23.65°C$, reduced the average heating load to $118.8\ kWh$, and extended the mechanical-free operational period by 26 hours compared to the height adjustment scenario. However, increasing the number of sides of the solar chimney to six demonstrated the most significant improvements, achieving an average indoor temperature of $24.2°C$, a peak heating load of $212.5\ kWh$, and a substantially lower average heating load of $48.9\ kWh$. Additionally, this configuration further extended the passive operation period by 9 hours compared to the outlet surface area scenario.

These findings demonstrate that increasing the number of sides of the solar chimney is the most effective method for reducing heating loads, improving thermal comfort, and enhancing energy efficiency. This effectiveness is due to the significant expansion of both the absorber plate surface area and the glazing, which together boost the solar chimney's performance, surpassing the benefits of increasing its height or outlet surface area. This research highlights the potential of integrating solar chimneys and Trombe walls with PCM to enhance energy performance in residential buildings. Future work can refine these technologies and explore their integration with modern HVAC systems for diverse climates.

REFERENCES

[1] Al-jarjary, Arkan Sabhan, Omer K. Ahmed, and Sameer Algburi. "Enhancement Methods for the Performance of Storage Solar Collectors: A Brief Review." *Results in Engineering* (2024): 102302.

[2] Firoozzadeh, Mohammad, Amir Hossein Shiravi, and Sahar Hodaei. "An experimental approach on employing air flow through a porous medium as coolant of photovoltaic module: thermodynamics assessment." *Thermal Science and Engineering Progress* 40 (2023): 101799.

[3] Meria, Firas Hussein, Sameer Algburi, and Omer K. Ahmed. "Impact of porous media on PV/thermal system performance: A short review." *Energy Reports* 11 (2024): 1803-1819.

[4] Dale, Spencer. "BP statistical review of world energy." *BP Plc: London, UK* (2021): 14-16.

[5] Ahmed, Omer K., Abdullah S. Hussein, Raid W. Daoud, and Zaid H. Ali. "A new method to improve the performance of solar chimneys." In *AIP Conference Proceedings*, vol. 2213, no. 1. AIP Publishing, 2020.

[6] Ahmed, Omer Khalil, and Abdullah Sabah Hussein. "New design of solar chimney (case study)." *Case studies in thermal engineering* 11 (2018): 105-112.

[7] Saleem, Ahmed Abdeen, Mahmoud Bady, Shinichi Ookawara, and Ali K. Abdel-Rahman. "Achieving standard natural ventilation rate of dwellings in a hot-arid climate using solar chimney." *Energy and Buildings* 133 (2016): 360-370.

[8] Rabani, Ramin, Ahmadreza K. Faghih, Mehrdad Rabani, and Mehran Rabani. "Numerical simulation of an innovated building cooling system with combination of solar chimney and water spraying system." *Heat and Mass Transfer* 50 (2014): 1609-1625.

[9] Shi, Long, Guomin Zhang, Wei Yang, Dongmei Huang, Xudong Cheng, and Sujeeva Setunge. "Determining the influencing factors on the performance of solar chimney in buildings." *Renewable and Sustainable Energy Reviews* 88 (2018): 223-238.

[10] Shi, Long, Guomin Zhang, Xudong Cheng, Yan Guo, Jinhui Wang, and Michael Yit Lin Chew. "Developing an empirical model for roof solar chimney based on experimental data from various test rigs." *Building and Environment* 110 (2016): 115-128.

[11] Saleem, Ahmed Abdeen, Mahmoud Bady, Shinichi Ookawara, and Ali K. Abdel-Rahman. "Achieving standard natural ventilation rate of dwellings in a hot-arid climate using solar chimney." *Energy and Buildings* 133 (2016): 360-370.

[12] Khayyaminejad, Amirhossein, and Amir Fartaj. "Unveiling the synergy of passive cooling, efficient ventilation, and indoor air quality through optimal PCM location in building envelopes." *Journal of Energy Storage* 89 (2024): 111633.

[13] Fernández-González, Alfredo. "Analysis of the thermal performance and comfort conditions produced by five different passive solar heating strategies in the United States midwest." *Solar Energy* 81, no. 5 (2007): 581-593.

[14] Raman, P., Sanjay Mande, and V. V. N. Kishore. "A passive solar system for thermal comfort conditioning of buildings in composite climates." *Solar energy* 70, no. 4 (2001): 319-329.

[15] Gonçalves, Helder, and João Mariz Graça. *Conceitos bioclimáticos para os edifícios em Portugal*. DGGE/IP-3E, 2004.

[16] Burek, S. A. M., and A. Habeb. "Air flow and thermal efficiency characteristics in solar chimneys and Trombe Walls." *Energy and buildings* 39, no. 2 (2007): 128-135.

[17] Fang, Xiande, and Yuanzhe Li. "Numerical simulation and sensitivity analysis of lattice passive solar heating walls." *Solar energy* 69, no. 1 (2000): 55-66.

[18] Chen, Wei, and Wei Liu. "Numerical analysis of heat transfer in a passive solar composite wall with porous absorber." *Applied Thermal Engineering* 28, no. 11-12 (2008): 1251-1258.

[19] Jiang, Bin, Jie Ji, and Hua Yi. "The influence of PV coverage ratio on thermal and electrical performance of photovoltaic-Trombe wall." *Renewable energy* 33, no. 11 (2008): 2491-2498.

[20] Ji, Jie, ChengLong Luo, Wei Sun, HanCheng Yu, Wei He, and Gang Pei. "An improved approach for the application of Trombe wall system to building construction with selective thermo-insulation façades." *Chinese Science Bulletin* 54, no. 11 (2009): 1949-1956.

[21] Shen, Jibao, Stéphane Lassue, Laurent Zalewski, and Dezhong Huang. "Numerical study on thermal behavior of classical or composite Trombe solar walls." *Energy and buildings* 39, no. 8 (2007): 962-974.

[22] Mezrhab, A., and M. Rabhi. "Modeling of the thermal transfers in an enclosure of the Trombe wall type." *Альтернативная энергетика и экология* 6 (2008): 9-14.

[23] Gan, Guohui. "A parametric study of Trombe walls for passive cooling of buildings." *Energy and buildings* 27, no. 1 (1998): 37-43.

[24] Drake, J. B. *A study of the optimal transition temperature of PCM wallboard for solar energy storage*. The Laboratory, 1987.

[25] Peippo, K., Pertti Kauranen, and P. D. Lund. "A multicomponent PCM wall optimized for passive solar heating." *Energy and buildings* 17, no. 4 (1991): 259-270.

[26] Kong, Xiangfei, Jinbo Li, Man Fan, Wei Li, and Han Li. "Study on the thermal performance of a new double layer PCM trombe wall with multiple phase change points." *Solar Energy Materials and Solar Cells* 240 (2022): 111685.

[27] Zhang, Yuan, Ziyang Zhu, Zian Peng, Jing Luo, Xiaoqin Sun, Jie Li, and Fen Peng. "The Trombe wall equipped with PCMs for the enhancement of the indoor thermal quality." *Energy and Buildings* 297 (2023): 113407.

[28] Mathur, Jyotirmay, and Sanjay Mathur. "Summer-performance of inclined roof solar chimney for natural ventilation." *Energy and Buildings* 38, no. 10 (2006): 1156-1163.

[29] Imran, Ahmed Abdulnabi, Jalal M. Jalil, and Sabah T. Ahmed. "Induced flow for ventilation and cooling by a solar chimney." *Renewable energy* 78 (2015): 236-244.

[30] Ellis, Peter Graham. "Development and validation of the unvented Trombe wall model in EnergyPlus." PhD diss., University of Illinois at Urbana-Champaign, 2003.